Multi-scale analysis of masonry panels based on mixed finite element formulations

Daniela Addessi, Vincenzo Ciampi, Maria Laura De Bellis, Achille Paolone
Department of Structural Engineering, Sapienza University of Rome, Italy
E-mail: daniela.addessi@uniroma1.it, vincenzo.ciampi@uniroma1.it,
marialaura.debellis@uniroma1.it, achille.paolone@uniroma1.it

Keywords: multi-scale models, masonry, mixed finite elements.

SUMMARY. A first order multi-scale model for regular masonry based on a periodic homogenization technique is presented. In particular, a two-field mixed finite element formulation is proposed for the solution of the boundary value problem at the macroscopic level, aiming at improving the accuracy of the macroscopic field evaluation. Some applications on simple 2D structures are shown both in the field of linear elastic and elastic-plastic behavior.

1 INTRODUCTION

In the last years computational homogenization techniques, based on multi-scale procedures, have caused a wide interest in the current scientific literature in various scientific fields, aiming at developing accurate models to reproduce the mechanical response of heterogeneous materials. In fact, they allow to strike a good balance between the achievement of detailed information at the constituents scale and the requirement of holding the computational costs down, when a structural problem involving a composite material is approached.
Recently, they have been satisfactorily employed in the modeling of masonry structural response, mainly in the case of regular textures ([1], [2]). The problem is split into two scales: a macro-scale, where an equivalent homogeneous continuum is considered for masonry, whose formulation is completely stated except for the constitutive law, and a micro-scale, in which all constituents are modeled in detail taking into account geometrical arrangement, size and constitutive laws of bricks and mortar joints. In particular, at the micro-level, a statistically representative volume element (RVE) of the actual masonry structure is defined. Therefore, whenever a constitutive information is required at each point of the macro-level, i.e. the relation between macroscopic deformation and stress components, it is necessary to get down to the lower level, where a boundary value problem (BVP) has to be solved in order to determine the microscopic stress field and the constitutive matrix. Then, the computed microscopic stress components and the constitutive matrix are homogenized and sent back to the macro-level. As for the BVP at the micro-level, periodic kinematic conditions are imposed on the RVE boundary, [3], derived on the basis of a suitable kinematic map linking the microscopic displacement fields to the macroscopic strain components.

In this paper a first-order multi-scale model for masonry is presented, where Cauchy continuum is employed at both the macro- and micro-scale. The solution of the two coupled BVPs at the two levels is evaluated by means of a Finite Element (FE) procedure. In literature, the proposed multi-scale models are mainly based on the classical displacement-based FE formulations. To this end, it has been widely recognized that mixed two- and three-field FE (derived on the basis of extended variational principles such as Hellinger-Reissner or Hu-Washizu) assure the overcoming of some well-known limits of the classical displacement-based formulations and the achievement of more accurate responses in terms of displacements and stresses ([4], [5], [6]), at least when adopted in the context of macroscopic models.

Aim of this work is to present a multi-scale approach where at the macro-level a two-field mixed FE formulation is adopted, while the classical displacement-based FE procedure is employed at the micro-level. The objective is to improve the effectiveness and the accuracy of the computational homogenization process, and, at the same time, to reduce the computational efforts by adopting coarser meshes at the macro-level. In fact, the higher performances of the mixed FE solution techniques result in a more accurate evaluation of the macroscopic stresses at each Gauss integration point, and, as a consequence, of the macroscopic strain components used as input data for the BVP at the micro-level. In particular, a class of Lagrangian mixed FE based on the one initially proposed in [5] and later on adopted in [7] for damaging materials. In the adopted mixed formulation it is assumed a standard Lagrangian expansion for the macro-level displacement field, while the stress field representation is defined by enforcing the satisfaction of a virtual work orthogonality condition with respect to a set of incompatible strain shape functions, properly selected. The use of such a formulation in the multi-scale framework is a good strategy to improve the performances of the method, both in linear and non-linear range. In particular, firstly some applications, classically presented in literature in the linear elastic regime, are presented to put in evidence the performances of the proposed mixed FE multi-scale procedure. Afterthat, the structural response of a masonry panel is analyzed, by adopting an elastic-plastic constitutive law for the mortar joints, able to reproduce the friction mechanism. The damaging behavior of the masonry constituents is herein neglected to avoid strain-softening behaviors and the associated numerical mesh-dependency problems.

2 MULTI-SCALE APPROACH

Conceptually, in the multi-scale procedure, every material point *P* of the equivalent homogenized domain Ω at the macro-level is linked to an underlying domain ω at the micro-level, the RVE, obtained by ideally enlarging the narrow zone around the point *P*. It is supposed that such a domain is periodically repeated in its neighborhood and undergoes periodic deformations.

Two BVPs are stated at both the macro- and micro-level. In particular, for each macroscopic material point, a nested BVP is formulated on the associated RVE. A mixed two-fields FE formulation for two-dimensional problems is here adopted, assuming displacements and stresses as independent fields. At the macro-level, denoting with Γ_t and Γ_u the portions of the boundary where tractions and displacements are applied, respectively, a weak form of the equilibrium and compatibility equations is stated as follows:

$$\int_{\Omega} (\mathbf{L}\,\delta\mathbf{U})^T\,\mathbf{\Sigma}\,d\Omega - \int_{\Omega} \delta\mathbf{U}^T\,\mathbf{B}\,d\Omega - \int_{\Gamma_t} \delta\mathbf{U}^T\,\mathbf{T}\,d\Gamma = 0 \quad in \quad \Omega \tag{1}$$

$$\int_{\Omega} \delta\mathbf{\Sigma}^T\,(\mathbf{L}\,\mathbf{U} - \mathbf{E})\;d\Omega = 0 \quad in \quad \Omega \tag{2}$$

with:

$$\mathbf{U} = \overline{\mathbf{U}} \quad on \quad \Gamma_u$$

where $\mathbf{U}$, $\mathbf{E}$ and $\mathbf{\Sigma}$ are the displacement, strain and stress vectors at the macro-level, respectively; $\mathbf{B}$, $\mathbf{T}$ and $\overline{\mathbf{U}}$ are the body forces, the applied tractions and the imposed displacements; $\mathbf{L}$ is the compatibility operator and δ indicates the variation of the quantity. In the spirit of the two-field mixed FE formulation, the constitutive relationship connecting $\mathbf{E}$ and $\mathbf{\Sigma}$ have to be enforced pointwise at each Gauss integration point of the macro-level. On the other hand, in the adopted multi-scale procedure the constitutive law is not directly available at the macro-level and it has to be obtained from the micro-scale level, by means of homogenization rules. In order to determine the

homogenized constitutive matrix and the macroscopic stress vector at each Gauss point of the macro-scale, a non standard BVP with periodic boundary conditions is solved on the RVE at the micro-level. Special conditions are, in fact, required in order to effectively formulate the scale transition procedure. The macroscopic strain measure $\mathbf{E}$ is the macro-level information passed to the RVE by means of a proper formulated kinematic map linking the displacement $\mathbf{u}$ at the micro-level to the macroscopic deformation components $\mathbf{E}$. Without loss of generality the *strain periodic* microscopic displacement field $\mathbf{u}$ may be written in the following form:

$$\mathbf{u}(\mathbf{x}) = \mathbf{E}\mathbf{x} + \mathbf{u}^p(\mathbf{x}) \tag{3}$$

where $\mathbf{E}$ is the macroscopic strain tensor, $\mathbf{x}$ is the position vector in the RVE and $\mathbf{u}^p(\mathbf{x})$ is a periodic micro-level fluctuation.

The displacement field, solution of the RVE, is thus obtained as the superposition of two different fields, the first one, $\mathbf{E}\,\mathbf{x}$, driven by the macro-level (i.e. the kinematic map imposed on the RVE boundary) and the second one, $\mathbf{u}^p(\mathbf{x})$, which is a local solution field respecting the periodicity between couples of periodic edges.

The classical equations of the displacement approach govern the BVP at the micro-level, except for the boundary conditions, which impose the periodicity of the displacement field and the anti-periodicity of the tractions on the boundary and are stated as follows:

$$\mathbf{u}^+ - \mathbf{u}^- = \mathbf{E}\mathbf{x} \tag{4}$$

$$\mathbf{t}^+ + \mathbf{t}^- = \mathbf{0} \tag{5}$$

where $\mathbf{u}^{+/-}$ and $\mathbf{t}^{+/-}$ are displacements and forces at periodic nodes on the RVE boundary. The constitutive laws for the constituents of the RVE have finally to be stated at the micro-level.

3 FINITE ELEMENT FORMULATION

As for the micro-level solution, a standard displacement-based finite element method is employed and 4-node quadrilateral elements are used for the discretization of the RVE. On the other hand, the mixed FE formulation, based on the independent expansions of displacement and stress fields, is adopted to solve the macro-level BVP. As for the selection of the displacement and stress shape functions, the approach proposed in (5) is followed. In particular, a continuous interpolation in the overall global domain Ω is adopted for the displacement, while an expansion which is continuous only within the individual finite element domain Ω^e is assumed for the stress field.

Then, the element displacement and stress functions in the element domain, $\mathbf{U}^e$ and $\mathbf{\Sigma}^e$, are represented as functions of n_v generalized displacement parameters $\mathbf{Q}^e$ and n_s stress parameters $\mathbf{S}^e$, as:

$$\mathbf{U}^e = \mathbf{N}_U\left(\mathbf{X}\right)\mathbf{Q}^e \tag{6}$$

$$\mathbf{\Sigma}^e = \mathbf{N}_S\left(\mathbf{X}\right)\mathbf{S}^e \tag{7}$$

where the matrices $\mathbf{N}_U$ and $\mathbf{N}_S$ collect the displacement and stress shape functions, and $\mathbf{X} \in \Omega^e$. In the following the natural coordinates $\boldsymbol{\xi} = (\xi, \eta)$ for isoparametric finite elements are used. While the standard displacement shape functions for Lagrangian quadrilateral finite elements of generic order k are contained in $\mathbf{N}_U$, selected in the Lagrangian polynomial space $\mathbf{P}_{k,k}\left(\xi, \eta\right)$, the stress expansion is chosen as:

$$\begin{aligned} \Sigma_{\xi\xi} &\in P_{k-1,k} \\ \Sigma_{\eta\eta} &\in P_{k,k-1} \\ \Sigma_{\xi\eta} &\in P_{k-1,k-1} \end{aligned} \tag{8}$$

where $P_{i,j}$ denote the scalar space containing all the Lagrangian polynomials of degree $\leq i$ in ξ and $\leq j$ in η.

By exploiting the approximations (6, 7) and by adopting a step-by-step technique with time step $\Delta t = t^{n+1} - t^n$, based on an implicit backward Euler difference scheme, to solve the incremental BVP at the macro-level, the mixed FE procedure is governed, at the macroscopic element level, by the following equilibrium and compatibility equations:

$$\mathbf{B}^e \ \Delta\mathbf{S}^{e,n+1} - \Delta\mathbf{F}_0^{e,n+1} = \mathbf{0} \tag{9}$$

$$\mathbf{B}^{e\,T} \ \Delta\mathbf{Q}^{e,n+1} - \Delta\mathbf{D}^{e,n+1} = \mathbf{0} \tag{10}$$

where Δ refers to the increment of the variables within the time step Δt. In (9) $\mathbf{B}^e$ is the element equilibrium matrix:

$$\mathbf{B}^e = \int_{\Omega^e} (\mathbf{L}\mathbf{N}_U)^T \ \mathbf{N}_S \ d\Omega^e \tag{11}$$

and $\Delta\mathbf{F}_0^{e,n+1}$ the increment of the equivalent nodal load vector:

$$\Delta\mathbf{F}_0^{e,n+1} = \int_{\Omega^e} {\mathbf{N}_U}^T \ \Delta\mathbf{B}^{n+1} \ d\Omega^e + \int_{\Gamma_t^e} {\mathbf{N}_U}^T \ \Delta\mathbf{T}^{n+1} \ d\Gamma^e \tag{12}$$

In (10) $\Delta\mathbf{D}^{e,n+1}$ represents the increment of the element generalized deformation vector, defined as:

$$\Delta\mathbf{D}^{e,n+1} = \int_{\Omega^e} \mathbf{N}_S^T \ \Delta\mathbf{E}^{e,n+1} \ d\Omega^e = \left(\int_{\Omega^e} \mathbf{N}_S^T \mathbf{C}_t^{n+1} \mathbf{N}_S \ d\Omega^e \right) \ \Delta\mathbf{S}^{e,n+1} = \mathbf{A}^{e,n+1} \ \Delta\mathbf{S}^{e,n+1} \tag{13}$$

where $\mathbf{C}_t^{n+1}$ is the tangent compliance matrix defined as:

$$\mathbf{C}_t^{n+1} = \left(\frac{\partial\mathbf{E}}{\partial\boldsymbol{\Sigma}} \right)^{n+1} \tag{14}$$

and $\mathbf{A}^{e,n+1}$ is the element tangent compliance matrix, $\Delta\mathbf{S}^{e,n+1}$ denoting the increment of the element stress parameters in the time step. Then, the compatibility equation (10) can be rewritten as:

$$\mathbf{B}^{e\,T} \ \Delta\mathbf{Q}^{e,n+1} - \mathbf{A}^{e,n+1} \ \Delta\mathbf{S}^{e,n+1} = \mathbf{0} \tag{15}$$

It has to be underlined that, since we are using a hybrid formulation, the compatibility equation has to be enforced separately on each element domain Ω^e, where the stress shape functions result C^0-continuous. By adopting a condensation procedure, the increment of the element stress parameters $\Delta\mathbf{S}^{e,n+1}$ can be expressed from the local compatibility equation (15) in terms of $\Delta\mathbf{Q}^{e,n+1}$ and substituted into the equilibrium equation (9), which results expressed in terms of the displacement parameters only. Since the displacement field is continuous everywhere in the structure, the equilibrium equation (9) can be enforced at the global level by applying the usual assembling procedure.

3.1 Solution algorithm

At each time step an iterative solution procedure is employed, with single iteration cycles for solving simultaneously the global equilibrium and the local compatibility equations. For each macroscopic iteration, the solution of the BVP at the micro-level is determined again by a Newton-Raphson iterative procedure. The main steps of the iterative procedures used are briefly described below.

In what follows, the apices $'^{n}'$ and $'^{n+1}'$, referring to the end points of the time steps, are omitted, while the apices $'^{k}'$ and $'^{k+1}'$ indicate previous and current iterations and δ denotes the increment of the variable at the iteration $'^{k+1}'$. The iterative scheme is based on the linearization of the element equations (9) and (15), which result:

$$\mathbf{r}_{eq}^{e,k+1} = \mathbf{r}_{eq}^{e,k} + \mathbf{B}^{e\,T}\,\delta\boldsymbol{\Delta}\mathbf{S}^{e,k+1} \tag{16}$$

$$\mathbf{r}_{c}^{e,k+1} = \mathbf{r}_{c}^{e,k} + \mathbf{B}^{e\,T}\,\delta\Delta\mathbf{Q}^{e,k+1} - \left(\frac{\partial\left(\mathbf{A}^{e}\Delta\mathbf{S}^{e}\right)}{\partial\Delta\mathbf{S}^{e}}\right)^{k}\delta\Delta\mathbf{S}^{e,k+1} \tag{17}$$

where $\mathbf{r}_{eq}^{e,k+1}$ and $\mathbf{r}_{c}^{e,k+1}$ are the residual vectors evaluated on the local equilibrium and compatibility equations, respectively, at the current iteration $'^{k+1}'$, while $\mathbf{r}_{eq}^{e,k}$ and $\mathbf{r}_{c}^{e,k}$ are the same vectors at the previous iteration $'^{k}'$. It has to be noted that, when a linear elastic behavior is considered, the last term in Eq. (17) vanishes. By imposing the vanishing of the compatibility residual Eq. (17), $\delta\Delta\mathbf{S}^{e,k+1}$ is evaluated and substituting into Eq. (16), so that a condensed residual equilibrium is obtained [ref. Grimaldi]. The standard assembling procedure is, then, applied to obtain the expression of the global equilibrium residual $\mathbf{r}_{eq}^{k+1}$:

$$\mathbf{r}_{eq}^{k+1} = \widetilde{\mathbf{r}}_{eq}^{k} + \mathbf{K}^{k}\,\delta\Delta\mathbf{Q}^{k+1} \tag{18}$$

where $\mathbf{K}^{k}$ is the global tangent stiffness matrix and $\delta\Delta\mathbf{Q}^{k+1}$ the iterative increment of the global displacement unknowns.

In the following the solution procedure is briefly described. By imposing the vanishing of the global equilibrium residual (18), the global vector $\delta\Delta\mathbf{Q}^{k+1} = -\mathbf{K}^{k}\,\widetilde{\mathbf{r}}_{eq}^{k}$ is first computed and, hence, the element vectors $\delta\Delta\mathbf{Q}^{e,k+1}$ and $\delta\Delta\mathbf{S}^{e,k+1}$ are evaluated.

In order to solve the iterative scheme defined by (16) and (17), a "*predictor - corrector*" procedure is adopted as follows:

- *predictor phase*

During the predictor phase, the last term of the right-hand side in (17) is simplified, since the element compliance matrix $\mathbf{A}^{e}$ is constant, and $\delta\Delta\mathbf{S}^{e,k+1}$ is evaluated as:

$$\delta\Delta\mathbf{S}^{e,k+1} = \mathbf{A}^{e,k^{-1}}\left(\mathbf{r}_{c}^{e,k} + \mathbf{B}^{e\,T}\,\delta\Delta\mathbf{Q}^{e,k+1}\right) \tag{19}$$

From $\Delta\mathbf{S}^{e,k+1} = \Delta\mathbf{S}^{e,k} + \delta\Delta\mathbf{S}^{e,k+1}$ the trial stress $\Delta\boldsymbol{\Sigma}^{e,k+1}$ at each Gauss integration point of the macro-level is computed, making use of the interpolation relation (7). Then, a trial evaluation of the macroscopic deformation vector at the Gauss point is performed by using the element compliance matrix at the previous iteration $'^{k}'$ and it follows:

$$\Delta\mathbf{E}^{e,k+1} = \mathbf{C}_{t}^{k}\Delta\boldsymbol{\Sigma}^{e,k+1} \tag{20}$$

- *correction phase*

The computed macroscopic strain components are now passed as input variables to the lower micro-level, where the iterative Newton-Raphson technique is used to solve the nonlinear FE problem on the RVE. As for the periodic boundary conditions (4, 5), the Lagrange multiplier method is adopted for the incorporation of these constraints into the computation of the equilibrium state of the microstructure, ending up with a set of nonlinear equations, where the unknown vector contains the nodal displacement degrees of freedom and the Lagrange multipliers representing the force acting on the node pairs of the boundary. After solving the finite element problem at the micro-level, the macroscopic stress components at the Gauss point are updated by applying the homogenization procedure. The compliance tangent matrix is evaluated by means of the procedure reported in (8). Such procedure is based on the partitioning of the displacement degrees of the discretized RVE into those of the interior domain and those associated with the boundary of the RVE. It is shown that the overall stresses and tangent moduli of a typical RVE may exclusively be defined in terms of discrete forces and stiffness properties associated with the displacement degrees of freedom on the boundary, by properly condensing the displacement degrees of freedom in the interior domain.

4 NUMERICAL RESULTS

In order to investigate the performances of the proposed mixed FE for the multi-scale model, compared with the results obtained by employing standard displacement-based FE, two numerical 2D applications are carried out.

4.1 Cook's Test

The first application is the so-called Cook's test in the linear elastic range. In Figure 1 the geometry and boundary conditions are shown. Geometrical dimensions are expressed in mm. The specimen is subjected to a vertical load p equal to $140kN$ applied at the right end.

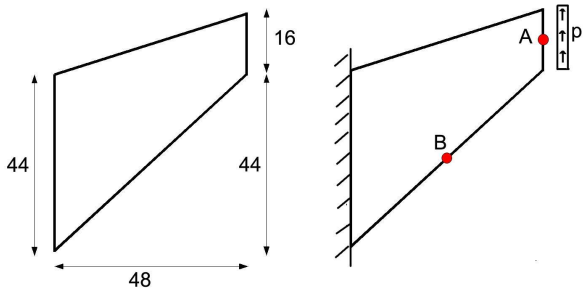

Figure 1: Cook's Test: geometry and boundary conditions.

Different 4-node, displacement-based (Q4) and mixed (M4), and 9-node, displacement-based (Q9) and mixed (M9), meshes have been adopted at the macro-level, as reported in Figure 2 . In the same Figure also the micro-level mesh is shown (constituted by 256 4-node rectangular FE). A unit square RVE has been considered, reproducing a multilayered material made of a hard core (HC) bounded by two soft layers (SL) characterized by the following elastic properties: $E_{HC} = 21000$ MPa, $\nu_{HC} = 0.3$; $E_{SL} = 1000$ MPa, $\nu_{SL} = 0.3$. The volume fraction of each component is 0.5. (MESH1 1 element; MESH2 4 elements; MESH3 16 elements; MESH4 81 elements; MESH5 100 elements) A convergence analysis is firstly performed in terms of displacements and stresses. In Figure 3, for the Q4, M4, Q9 and M9, the vertical displacement corresponding to point A in Figure

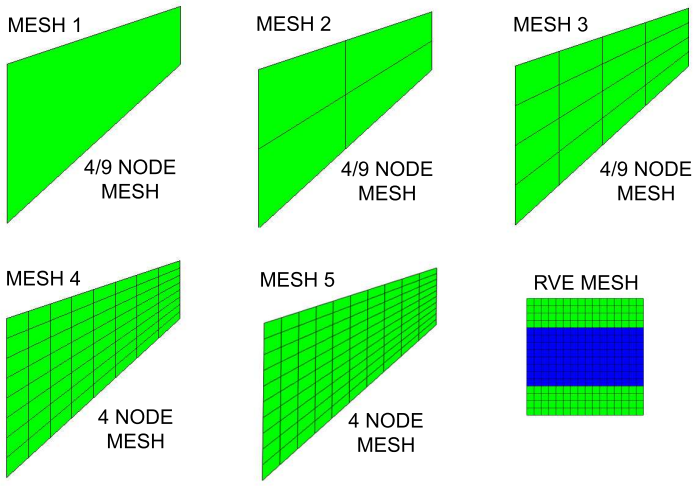

Figure 2: Cook's Test: adopted 4/9 node macro-level meshes and RVE mesh.

1, is plotted for each adopted mesh. The values of the displacements are normalized with respect to the reference value, corresponding to the one evaluated by the finest M4 mesh. It is clear that the mixed elements exhibit faster convergence properties: already with MESH3, M4 attains the value 0.97, showing a better performance than Q4 and Q9. The best results are obtained with M9 for which the reference converged value is obtained with MESH3. Similarly in Figure 4 the convergence is analyzed for the vertical stress Σ_B calculated at the integration point nearest to point B in Figure 1. Again, it is possible to appreciate the improved behavior of M4 with respect to Q4.

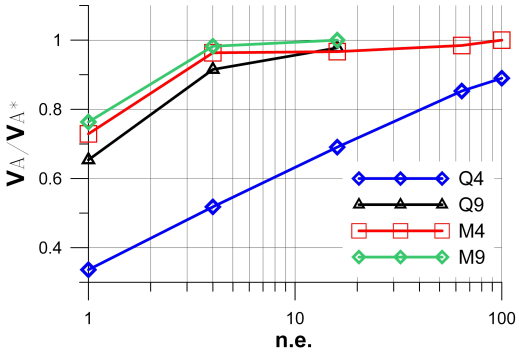

Figure 3: F.E. convergence: Point A vertical displacement

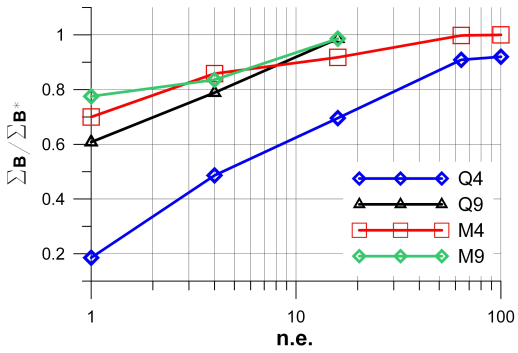

Figure 4: F.E. convergence: Point B vertical stress.

4.2 Wall with openings

The example consists in the numerical simulation of the linear and non-linear behavior of a regular brick masonry wall with openings, whose geometry and boundary conditions are shown in Figure 5. A lateral triangular emi-symmetric load (the resultant of the distribution is equal to 15

kN) is applied and the horizontal δ_1 and δ_2 displacements are monitored as shown in Figure 5. The

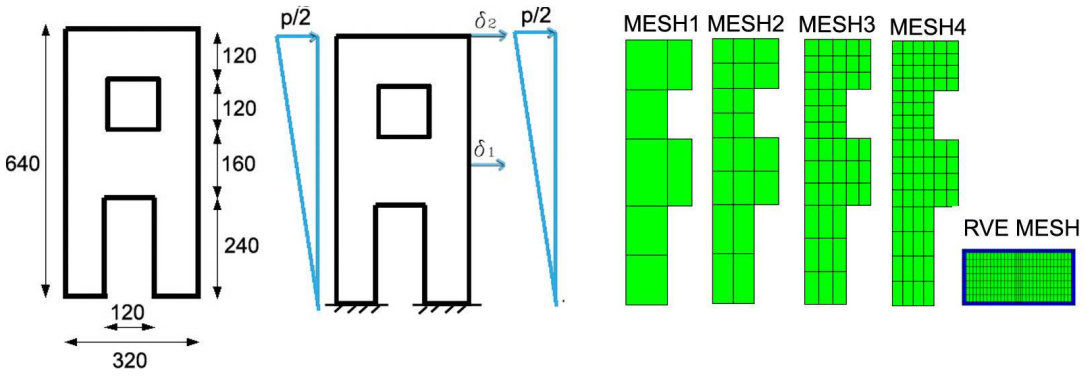

Figure 5: Wall with openings: geometry and boundary conditions (left); macro and micro-level adopted meshes (right).

analyses are carried out using, at the macro-level, four different meshes of 4-node rectangular FE (Q4 and M4) (MESH1 7 element; MESH2 20 elements; MESH3 40 elements; MESH4 80 elements); due to emi-symmetry conditions of the problem, only one half of the structure is considered (see Figure 5). A stacking bond arrangement of the masonry blocks is supposed, thus the adopted RVE consists of one block (140x65x100 mm^3) surrounded by $5mm$ thick half mortar joint (the adopted FE mesh is shown in Figure 5). Firstly, the response in the linear elastic regime is investigated. The mechanical parameters are $E_b = 5500\ MPa$ and $\nu_b = 0.2$ for the brick and $E_m = 1500\ MPa$ and $\nu_m = 0.25$ for the mortar. In Figure 6 the vertical strain distributions are shown both for Q4 and M4 and for the different adopted meshes. It appears that M4 provides a more accurate response already for very coarse meshes, while Q4 and M4 give very similar distributions in the case of the finest meshes. In Figure 7 the structural response is examined in terms of the normalized displacements δ_1/δ_1* and δ_2/δ_2* versus the adopted number of elements (n.e.). The displacement evaluated with MESH4 M4 is assumed as the "reference" value. M4 show a better behavior than the displacement-based FE for all the considered meshes and for both the considered displacements. The finer is the mesh, the smaller are the differences between Q4 and M4: in the case of MESH1, in fact, the respective percentage difference for δ_1/δ_1* is about 20%, while for MESH4 it decreases up to 8%. Afterthat, the non-linear structural response of the wall is analyzed: the linear elastic constitutive law is assumed for the bricks, while a Von-Mises plasticity model with isotropic hardening, which accounts for different material strengths in tension and compression, is considered for mortar joints. No damaging mechanical behavior is taken into account, in order to avoid strain-softening responses and pathological numerical mesh-dependency. The used elastic parameters for bricks and mortar are the same as before, while the plastic parameters are: the yield threshold in compression is imposed equal to $4.2\ MPa$, the yield threshold in tension is equal to $0.36\ MPa$ and the hardening coefficient is 0.15. In Figure 8 the applied horizontal load resultants versus the displacements δ_2 for the different meshes considered and for Q4 (left) and M4 (right) are reported (the plot is stopped at the point nearest to a displacement of $1.4mm$). The better convergence properties of the mixed elements are clearly shown and the "reference" curve (M4 MESH4) is approached, respectively, from above or from below.

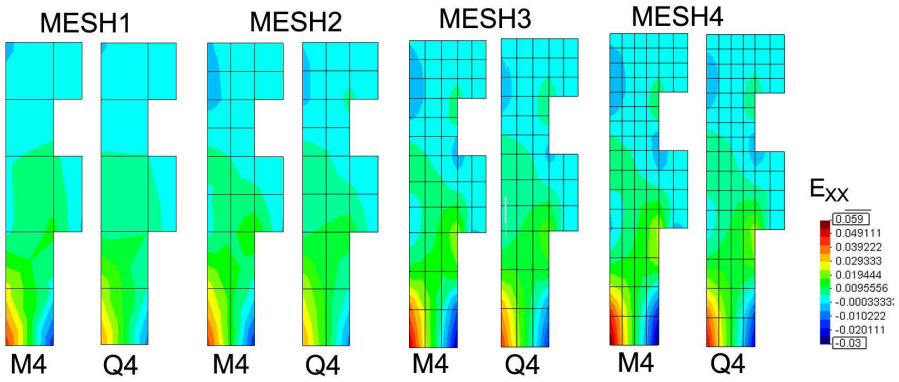

Figure 6: Comparison between displacement based and mixed finite element formulations: vertical strain distribution (corresponding to the four adopted meshes).

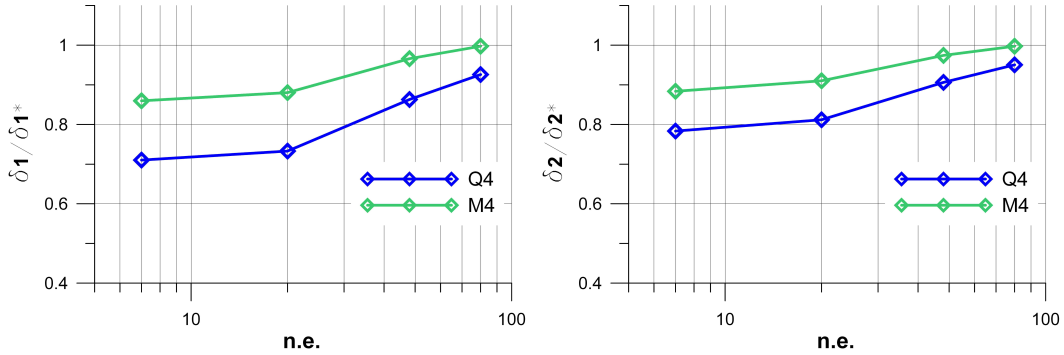

Figure 7: Linear elastic case: horizontal displacement, normalized with respect to the converged value, versus number of elements for displacement based 4-node elements (Q4) and mixed 4-node elements (M4) meshes.

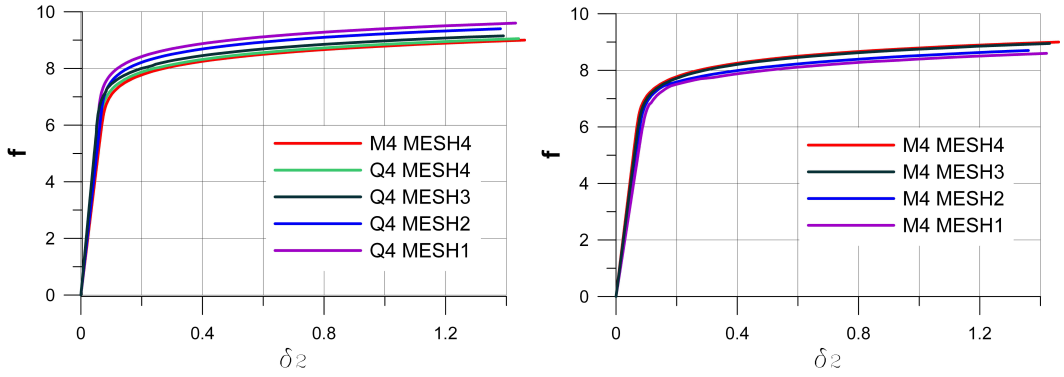

Figure 8: Elastic-plastic case: applied horizontal load resultant versus the displacement δ_2 for the different meshes considered and for the Q4 (left) and M4 (right) elements.

5 CONCLUSIONS

A first order multi-scale model based on a periodic homogenization procedure has been presented for modeling 2D masonry structural response. In particular, a mixed FE formulation has been proposed to solve the macro-level BVP, based on the independent expansion of the displacement and stress macroscopic fields. Some numerical applications on 2D simple structures have been performed by adopting a linear elastic, as well as an elasto-plastic constitutive behavior for the constituents at the micro-level. The analysis of the convergence properties of the presented enhanced FE formulation, compared with a classical displacement-based approach, clearly have shown the better performance of the mixed FE method both in the linear and nonlinear range. In fact, it gives more accurate results in terms of global response quantities and in reproducing the stress distributions in the analyzed structures. The iterative Newton-Raphson algorithm implemented together with the iterative predictor-corrector procedure adopted at the micro-level has shown good robustness and effectiveness properties.

References

[1] T. J. Massart. *Multiscale modelling of damage in masonry structures*. PhD thesis, Technische Universiteit Eindhoven, 2003.

[2] T.J. Massart, R.H.J. Peerlings, and M.G.D. Geers. An enhanced multi-scale approach for masonry wall computations with localization of damage. *International Journal for Numerical Methods in Engineering*, 69(5):1022–1059, 2007.

[3] R. J. M. Smit, W. A. M. Brekelmans, and H. E. H. Meijer. Prediction of the mechanical behaviour of nonlinear heterogeneous systems by multi-level finite element modeling. *Computer Methods in Applied Mechanics and Engineering*, 155:181–192, 1998.

[4] T.H.H. Pian and K. K. Sumihara. Rational approach assumed stress finite elements. *Int. J. for Numerical Methods in Eng.*, 20:1685–1695, 1984.

[5] M. Bischoff, Ramm E., and D. Braess. A class of equivalent enhanced assumed strain and hybrid finite element. *Computational Mechanics*, 22:443–449, 1999.

[6] A. Bilotta and R. Casciaro. Assumed stress formulation of high order quadrilateral elements with an improved in-plane bending behsviour. *Comp. Methods in Appl. Mech. and Eng.*, 191:1523–1540, 2002.

[7] R. Grimaldi, D. Addessi, and V. Ciampi. Localization and regularization behavior of mixed finite elements for 2d structural problem with damaging materials. *Computer Methods in Applied Mechanics & Engineering*, 197:255–264, 2007.

[8] C. Miehe and A. Koch. Computational micro-to-macro transition of discretized microstructures undergoing small strain. *Arch. Appl. Mech.*, 72:300–317, 2002.